IIETA International Information and Engineering Technology Association
Advancing the World of Information and Engineering

Traitement du Signal
Vol. 42, No. 3, June, 2025, pp. 1265-1277
Journal homepage: http://iieta.org/journals/ts

Reliable Low Power Wide Area Networks-Aided Polar Code

Muteb Alsaqhan[1,2], Abdulah Aljohani[3], Maazen Alsabaan[1*]

[1] Department of Computer Engineering, College of Computer and Information Sciences, King Saud University, Riyadh 11543, Saudi Arabia
[2] Next Gen Connectivity & Wireless Sensors Institute, King Abdulaziz City for Science and Technology (KACST), Riyadh 11442, Saudi Arabia
[3] Department of Electrical and Computer Engineering, King Abdulaziz University, Jeddah 21589, Saudi Arabia

Corresponding Author Email: malsabaan@ksu.edu.sa

https://doi.org/10.18280/ts.420305

Received: 23 June 2024
Revised: 28 August 2024
Accepted: 12 March 2025
Available online: 30 June 2025

Keywords:
Low Power Wide Area Network (LPWAN), Long Range Wide Area Network (LoRaWAN), Internet of Things (IoT), Forward Error Correction (FEC), Additive White Gaussian Noise (AWGN), Likelihood Ratio (LR), Lower Density Parity Check (LDPC), Successive cancellation decoding (SCD)

ABSTRACT

Low Power Wide Area Network (LPWAN) has emerged recently as a new IoT technology that offers wide coverage connectivity with low power consumption. However, this extraordinarily wide range and low-power performance come at the expense of high latency and low data rate. In 2008, Erdal Arkan proposed a new technique in the forwarding error correction mechanism, called polar codes, which offer a unique advantage of achieving channel capacity with low encoding and decoding complexity, scalability, and a low error floor, making them a compelling choice for error correction compared to other techniques. We used the polar codes mechanism in the LPWAN protocol to enhance error rate and data rate transmission. The performance of our approach demonstrated that polar codes can achieve an improved bit error rate at low data rates compared to the Hamming code technique used in LPWANs. For example, at 125 kHz, the Polar Codes signal-to-noise ratio outperforms the Hamming code used in LPWAN by 18 db. We can observe that at Spreading Factor 8, the Signal to noise ratio showed a better performance for our new code, polar code, with LPWAN for an error rate of 10^{-5}.

1. INTRODUCTION

With the rise of Internet of Things (IoT) and Machine-to-Machine (M2M) communication, IoT applications demand low power consumption to ensure energy efficiency within scalable networks. However, existing wireless technologies like IEEE 802.11 WLANs, though designed for high-speed data transmission, are power-intensive. Meanwhile, technologies such as IEEE 802.15.1 Bluetooth and IEEE 802.15.3 ZigBee offer lower power consumption but are limited by short-range capabilities.

To address the requirements of IoT applications, Low Power Wide Area Networks (LPWANs) have emerged as a class of wireless communication standards characterized by their ability to cover extensive areas. LPWANs are specifically designed to maximize range while minimizing power usage. However, this trade-off results in lower data rates and modest throughput, which are sufficient for long-distance communication spanning several kilometers [1, 2].

Substantial research has been conducted to evaluate the performance of LoRa and other LPWAN technologies, with most studies focusing on determining physical layer specifications through comprehensive field experiments [3, 4]. Despite these efforts, a significant gap remains in the literature concerning the analysis of the orthogonal chirp spread spectrum.

specifically, while some insights into achieving orthogonal symbols via the utilization of both up and down-chirps are provided by Reynders and Pollin [2], a comprehensive examination of the effects of interference and noise is conspicuously absent. This paper aims to address the research gap by exploring the potential of a Forward Error Correction (FEC) mechanism, named polar codes, as a coding technique to enhance the data rate in LPWANs. Polar Codes have been proven to achieve Shannon's Capacity for a symmetric binary-input discrete memoryless channel. Shannon Capacity is known as the maximum rate at which information can be transmitted over a channel as represent of the theoretical limit. To achieve Shannon capacity Polar Codes utilize a process called channel polarization and achieve the capacity by selecting sub-channels for transmission. By employing LPWAN Chirp Spread Spectrum modulation in the method, thereby facilitating a more reliable communication link. A particular emphasis is placed on assessing the coexistence of LPWAN technologies within this framework.

1.1 Problem statement

LPWAN aims to complement the present IoT market by offering a unique aspect of wide-area connectivity while maintaining the end-devices' power consumption and ensuring the cost is minimal. However, this significant performance comes with the expense of low data rate, low reliability, and high latency. The expectation of the use of LPWAN in the

present day is significantly important as all sensors and devices can be connected to one large network. However, the importance of the use of the LPWAN demands a high use of data sharing through networks and requires reliability in big data sharing. This cannot happen with a low data rate and high latency. Our research aims to enhance the data rate, reliability, and latency of LPWAN by employing novel Polar code algorithm techniques in LPWAN protocol. The study of our work shall generate an output of our deployment in enhancing the data rate of LPWAN protocol.

1.2 Background

We will briefly explain more about the IoT and LPWAN. We'll also cover technologies like NB-IoT, Sigfox, and LoRa, as well as polar codes. As the IoT being the technology to connects devices to the internet so they can collect and share data. LPWAN is a technology that helps these devices communicate over long distances without using much power. Technologies like NB-IoT, Sigfox, and LoRa are all different types of LPWAN. They help devices, like sensors, send data across wide areas. Polar codes are a new way to make sure the data they send is accurate and secure. We'll go into more detail on all these topics.

The advent of the IoT in 2010 marked a significant milestone in the evolution of networked devices, with the concept being strategically positioned to incentivize sensor developers towards the integration of diverse devices within a singular network framework. The scope of applications envisioned for the IoT has been expansive and, at times, beyond initial expectations, encompassing domains such as smart homes, smart cities, and beyond—each contributing to the burgeoning field of sensor technology [5, 6]. Ericsson has projected a substantial increase in IoT-connected devices, anticipating a surge to 20 billion by the year 2023, reflecting the rapid growth and integration of IoT within various aspects of modern life [7].

The IoT's operational efficacy is contingent upon its robustness and the capability to provide extensive coverage. The vast majority of IoT devices are designed for battery operation, with an operational lifespan objective ranging between five to ten years, thereby negating the necessity for frequent maintenance. This design philosophy enables IoT networks to extend their reach over large geographical expanses, facilitating widespread data collection and connectivity [8].

The architectural foundation of the IoT is predicated on the interconnection of a multitude of sensors, forming an extensive wide-area network that operates under a variety of technological protocols. This interconnectedness permits an extensive array of devices to communicate and share data, which can then be harnessed for various purposes, such as research analysis, analytical reporting, or real-time monitoring, contingent upon the specific application deployed. Ultimately, the primary goal of IoT infrastructure is to amalgamate data from diverse sources into a unified network, thereby empowering network designers and end-users to make informed decisions based on the consolidated information.

The LPWAN protocol represents an exemplar of operational efficiency, providing expansive coverage while maintaining significantly lower energy consumption in comparison to current technologies such as Zigbee, Bluetooth Low Energy (BLE), and Near Field Communication (NFC) [6]. LPWAN's operational paradigm is founded on the principle of transmitting data across extensive distances via wireless communication links while maintaining minimal power usage. The distinctive advantage of this technology lies in its capacity to provide extensive wireless range capabilities concomitant with low power consumption, rendering it particularly advantageous for activities involving monitoring and data analysis. In addition, when contrasted with the investment-heavy cellular networks, which demand complex infrastructure and transmission systems, LPWAN offers a cost-effective solution [9].

As illustrated in Figure 1, the IoT ecosystem encompasses a plethora of applications that demand both low power usage and long-range capabilities, such as water metering, smart home technology, and healthcare delivery systems. Various technologies exist within the LPWAN domain, including LoRa, Sigfox, and NB-IoT, each carving its unique niche within the broader IoT market. This paper will succinctly present an overview of these technologies and offer a comparative analysis of their channel codes, as delineated in Tables 1 and 2.

Figure 1. IoT type of application

LoRa (Long Range) technology, a prominent player in the IoT landscape, is acclaimed for its proficiency in facilitating communication over long distances while operating at a low data rate. This technology operates at the physical layer and is structured based on the principles of spread spectrum technology. LoRa employs a modulation scheme that efficiently disperses a signal to extend coverage across a broad network area. The versatility of the technology is further enhanced by the adoption of six distinct spreading factors, allowing for a strategic balance between data rate and range, a critical consideration in wireless communication [10].

The data transmission rates of LoRa can vary from as low as 300 bits per second (bps) to as high as 50 kilobits per second (kbps), a range that is influenced by the chosen spreading factor [11]. While LoRa is intrinsically associated with the LoRaWAN protocol—a Medium Access Control (MAC) layer protocol that builds upon LoRa's physical layer capabilities—it is important to recognize that the extensive coverage and low power consumption advantages provided by LoRa typically result in lower data rates [12].

These diminished data rates, however, introduce certain limitations, such as potential data loss, decreased throughput, and, at times, an unsustainable link for certain applications. This trade-off is a critical consideration for developers and users of LoRa technology when assessing its suitability for different IoT applications [13].

Sigfox emerges as an alternative LPWAN network operator within the IoT sector, distinguishing itself through its unique approach to connectivity. Adopting an end-to-end communication model, Sigfox enables endpoint devices to

transmit data directly to the connected base stations [14]. Unlike LoRa, Sigfox utilizes Binary Phase Shift Keying (BPSK) as its modulation technique. This method employs an ultra-narrow bandwidth of 100 Hz, an intentional design choice made to enhance frequency efficiency and thus reduce power consumption during operations [15].

The use of BPSK modulation in Sigfox allows for a maximum data rate of up to 100 bps. This is notably lower when compared to the data rate potentials of LoRa. Additionally, the payload capacity of Sigfox is limited to 12 bytes, which contrasts with LoRa's significantly larger payload capacity of up to 243 bytes [16]. This comparison underscores the critical trade-offs between different LPWAN technologies in regard to data rate and payload size, which are essential factors when considering the appropriateness of each technology for specific IoT applications [17].

Narrowband IoT (NB-IoT) is a LPWAN technology that builds on existing cellular protocols, such as third-generation (3G) and Long Term Evolution (LTE) standards, to enable IoT connectivity [18]. In terms of network architecture and operational principles, NB-IoT shares many characteristics with traditional cellular communication systems [12].

Unlike LPWAN technologies such as LoRa and Sigfox, NB-IoT uses single-carrier Frequency Division Multiple Access (FDMA) and Orthogonal FDMA (OFDMA) for its air interface. These techniques, commonly utilized in cellular networks, have been adapted within NB-IoT to address the specific requirements of IoT communication [19]. For modulation, NB-IoT employs Quadrature Phase-Shift Keying (QPSK), a reliable and efficient scheme recognized for its robustness [20].

The data rate capabilities of NB-IoT are considerable, with the potential to achieve up to 200 kilobits per second (kbps). Additionally, NB-IoT supports a larger payload size compared to its LPWAN counterparts, allowing for up to 1600 bytes of data to be transmitted [21]. This substantial data rate and payload capacity make NB-IoT a formidable option for IoT applications that demand higher throughput and more data-intensive operations [22].

Table 1. Comparison of IoT technologies [23]

	LoRa	**Sigfox**	**NB-IoT**
Third-Party infrastructure	Open Source	Open Source	Open Source
Operating Band	ISM Sub-GHz	ISM Sub-GHz	Licensed LTE band 180Khz
Channels	Multi SF 72 UL and 8 DL	360 Channels	3 DL and 2 UL
Modulation	CSS, FSK	DBPSK, GFSK	OFDMA, SC- FDMA
Data Rate	0.3 to 37.5 Kbps	100 bps UL 600 bps DL	Up to 250 kbps
Communication Range	5Km to 15Km [14, 24]	1Km to 5Km	Up to 35Km
Payload Length	250 B	12 B UL 8 B DL	1600 B
Authentication	Symmetrical Authentication Key	Burnt-in Symmetrical Authentication Key	Mutual Authentication
Encryption	AES 128bit	Without	LTE Encryption

Table 2. Comparison of coding technique of IoT technologies

	LoRa-Hamming	**Sigfox-DPSK**	**NB-IoT Turbo**
Pros	Simplicity	Simplicity	Provide high reliability
	Effective with a data stream	No need for carrier frequency	Power efficiency for moderately
Cons	Unreliability Low	Unreliability	Requires large frame length, high complexity
	Data Rate	Low Data Rate	Low Data Rate

Polar Code is an FEC mechanism. It has its construction based on symmetric binary input channels [25]. Polar Code was recently discovered by Arikan [26]. It aims to enhance the performance of a bit transmitted in the air to reduce the error of the bit transmitted. Many applications can be located using Polar Codes in the Software Defined Radio and Wireless Communication System. The construction of polar codes relies on the recursive application when using a successive Cancellation Decoding (SCD) to converge on either noiseless or purely noisy channels. Polar Codes have been found to achieve channel capacity, offering the advantage of modest encoding and decoding complexity reduction of (N log N), where N is the block length [27].

Polar Code complexity reduction can be achieved by recognizing and comprehending the special nodes in the decoding tree. The decoding tree is defined by the block length of the transmission. However, Successive Cancellation Decoding (SCD) relation to the reduction of the complexity is also based on the code length and list size L, which is (N log N). The improvement of list decoders is proportional to the list size, which is fixed even if the Signal to Noise Ratio (SNR) is high. Moreover, one of the other schemes helping in the reduction of the complexity is the path splitting operation in SCD, reducing the complexity of the decoding tree. The mitigation of complexity can be resolved in fast decoding, thereby reducing the latency of the decoded bits.

The successive cancellation list (SCL) decoding algorithm is an approach that enables polar codes to attain strong error-correction capabilities. Despite this, existing SCL algorithms and decoders primarily rely on likelihood ratios (LR), which result in significant hardware complexity. The work of SCL at the receiver end, where the transmitted codeword x is corrupted to a received codeword $y = (y1, y2, \dots yn)$. With the use of the LR of yi, a deterministic SC decoder performs decoding procedure to recover u [28].

2. LLITERATURE REVIEW

LPWAN has been highly developed in areas such as AI, machine learning, data analytics, and blockchain technologies. There is tremendous potential for exponential growth in regard to the deployment in several applications among different sectors of society, professions, and industries. The application of the IoT requires energy-efficient and low-complexity nodes for a variety of uses that are to be deployed on scalable

networks.

As the IoT continues to advance, the need for a long-range, low-power connectivity standard has started to hinder its progress. While technologies like Bluetooth Low Energy and Zigbee have successfully met the demands of the short-range, low-power device market, the current ecosystem offers limited solutions designed for devices requiring extended range alongside strict low-power operation. Recent advancements in communication technologies have highlighted the pivotal role of Long Range Wide Area Network (LoRaWAN) in bridging the energy harvesting gap by providing comprehensive long-range communication solutions. LoRaWAN is recognized for its low power consumption, extensive range, cost-effectiveness, security, and scalability, making it an ideal connectivity solution for both public operators and private networks, particularly in the context of IoT applications. Prior studies have underscored its effectiveness in various IoT scenarios, yet it is important to note that LoRaWAN's bandwidth limitations stem from challenges in its coding techniques. Specifically, its architecture employs spread spectrum modulation based on the LoRa physical layer, which, while beneficial for reducing power consumption and extending range, imposes constraints on bandwidth. Nonetheless, research indicates that devices leveraging LoRaWAN can operate on battery power for up to one year, maintaining robust performance even in indoor environments. The security used in LoRa WAN is based on the 128-bit Advanced Encryption Standard (128- AES) encryption. Nevertheless, it enables free location GPS applications related to its spread spectrum and timestamp.

LPWAN, which was introduced as a solution to the predicaments of limited range and high energy expenditure endemic to conventional IoT technologies, strives to augment the existing IoT framework. It proposes a unique proposition in the IoT landscape, ensuring wide-area connectivity without the burden of excessive power consumption or prohibitive costs [2]. Contrary to the traditional short-range, non-cellular IoT platforms such as Zigbee, Bluetooth, and Wi-Fi, LPWAN infrastructure is capable of delivering coverage that is superior in scope through a single gateway.

LPWAN protocol in the IoT environment has been unique for its ultra-wide connectivity for link capacity enhancement by +20dB [29]. The enhancement is capable of reaching a range of tens kilometers [15]. As stated before, LPWAN advantages come in their low-cost connectivity and large area coverage [30].

Moving forward with the system architecture and protocols are developed by LoRa Alliance [24]. LoRa Alliance is an open, nonprofit association that focus on spanning a wide range of players from chip makers to cloud provider such as Amazon. LoRa Alliance is considered one of the fast-ever-growing ecosystems. The LoRa Alliance facilitates a certification program and maintain interoperability specification in public.

The foundational architecture of LoRaWAN begins with its link-layer specification. Positioned above the LoRa physical layer and below the application layer, the link layer functions as the intermediary between end devices and the network. Acting as an over-the-air transport layer, it ensures that end devices can both transmit and receive application-layer payloads to and from the network. This layer includes key physical layer parameters, such as channel frequency, data rate, and transmission power.

Before delving deeper into the specifics of the link layer, it is important to highlight one of LoRaWAN's primary objectives: creating low-cost devices capable of operating for 5–10 years without requiring maintenance. This is achieved through cost-effective hardware design and maintaining minimal transmission power.

LoRaWAN networks are typically designed in a star-of-stars topology, where gateways serve as intermediaries, relaying packets between end devices and a central network server. Unlike conventional systems, this design does not rely on fixed links between devices and gateways, enabling uplink transmissions to be received by multiple gateways simultaneously.

Communication between end devices and gateways utilizes frequency shift keying (FSK) and LoRa modulation, which disperses transmissions across multiple frequency channels and data rates. In LoRaWAN, data rates range from 0.3 to 50 kbps, striking a balance between communication range and packet transmission time. Lower data rates enhance communication range but require more airtime, whereas higher data rates decrease airtime usage at the cost of increased power consumption, leading to reduced battery life.

Devices operating at varying data rates, however, do not interfere with each other. To enhance both battery performance and overall network efficiency, the LoRaWAN infrastructure dynamically manages the data rate and output power for each device through an adaptive data rate (ADR) mechanism.

The adaptive data rate (ADR) mechanism primarily relies on the distribution of gateways within the network. ADR allows gateways to capture uplinks from any device, enhancing the network's connectivity level and increasing receive redundancy. Recent studies, however, have explored the use of higher-order modulation techniques [31]. In essence, devices can transmit over any available channel at any time using any permitted data rate, provided the following conditions are met:

Devices switch channels in a pseudo-random manner for each transmission, improving robustness against interference.

Each device adheres to the maximum transmit duty cycle specific to its sub-band.

Devices comply with the maximum transmission duration allowed for their sub-band.

LoRaWAN devices typically follow an ALOHA-like communication protocol and may function in one of three operating classes.

Class A Devices: These devices are bidirectional and operate using an ALOHA-type protocol, where transmission slots are allocated based on individual communication demands, with minor random adjustments. After each uplink transmission, two brief downlink receive windows are available. This system operates with low power, making it suitable for applications that need downlink communication from the Network Server (NS) immediately following an uplink transmission. For other downlink communications, the next scheduled uplink must be awaited.

Class B Devices: Also bidirectional, these devices provide additional receive slots compared to Class A. Alongside the random receive windows, Class B devices feature scheduled receive slots enabled by time-synchronized beacons sent from a gateway.

Class C Devices: These bidirectional devices maximize receive opportunities by keeping receive windows nearly always open, only closing during transmissions. Although they consume more power than Class A or B devices, they

significantly reduce latency for communication from the server to the device. Devices can alternate between Class A and Class B operation modes as required. Each one of these classes has advantages among battery lifetime and downlink network communication latency. For instance, class A is the most energy efficient and is supported by all devices; however, downlink is only available after sensor transmission. Concerning class B, the battery powered actuators are also energy efficient, and latency-controlled downlink and slotted communication is synchronized with end devices. Lastly, Class C are also powered actuators with devices that can listen continuously; however, there is no latency for downlink communication.

Compared to cellular networks that have their communication coding scheme, like turbo codes used in the third generation, LPWAN has lower cost and less complexity [32, 33]. We can find LPWAN has its own coding scheme but with a low data rate due to the coding technique. We aim to enhance LPWAN by using other coding schemes such as Polar Codes that can improve the data rate compared to a cellular network, by using high order coding. The majority of the LPWAN technologies use different bands from 1 sub GHz [34] up to 2.4 sub GHz and is predominantly used by 2.4 sub GHz for less attenuation and multipath fading [14]. The majority used IoT technologies for environment evaluation study are LoRaWAN either indoor [30] or outdoor [35].

Polar Code has an explicit construction. The benefit of using Polar Code is that it is suitable for the control channel. The performance is poor to Low-Density Parity Check (LDPC) and turbo coding techniques [36]. Polar Code can achieve near high- performance capacity. To achieve a valuable performance, the codes attain to achieve the capacity by using a binary-input memoryless and symmetric channels. The use of the inputs must follow with efficient encoding and decoding algorithms. Other research adapted error control coding approaches for wireless communication systems in Polar Codes [37]. The construction relies on the recursive model and application type. The construction can combine successive-cancellation decoding and the binary-input symmetric channel like other coding techniques such as Convolutional Coding and LDPC. The goal of the Polar Code is to control the errors in data transmission within an unreliable or noisy channel. This technique works by redundantly encoding the transmitted message. This mechanism allows the receiver to detect the error bits and remove it from the original message. The order to perform Polar Coding is to have any information that can be formalized by the length of information sequence *N* that shall be transmitted as bits. The bits will be submitted in two forms, $u1$ and $u2$, for the structure encoder when $N = 4$. To obtain the output of our codeword, it shall be denoted as *X* where it is simply expressed mathematically as $u1 \oplus u2 \oplus u3 \oplus u4$ and can be further represented as: *X' = u'G*, where *G* is the generator matrix for $N = 4$, which we explained earlier. Polar code has its recursive structure as these are two techniques introduces for the encoder structures, which will be studied further in the future for performance enhancement by using these techniques. To achieve the goal of implementing Polar Coding we shall have a generator matric for the encoder part. In the construction of encoding, we shall have one matrix for $N = 4$ and the bits are in $u_1u_2\ u_3u_4$ where the data bit vector is explained in $u_1^N \dots u_i^N$ and for a codeword to achieve the polar coding, we must have it as follow $X_1^N = u_1^N G_n$ [28]. Where the generator matric can be obtained by $G_n = B_nF \oplus N$ G_n=B_n *F^XOR n* where is the B_n can be calculated as $B_n = R_n(I_2 \oplus B_n)$ where the initial B_n denotes the $N \times N$ reverse shuffle permutation matrix defined. Other authors have a different opinion in working with metrics permutation, which will necessitate further investigation and study. Polar Codes was recognized for finding the probability of bit error in split memoryless channels, as opposed to using algebraic methods. Arikan proposed using Bhattacharyya Parameter in finding the error decision in a certain bit called the determination of a frozen bit location in the Polar Code. Bhattacharyya Parameter in Polar Codes aims to find the erasure probability channel. The Bhattacharyya parameter can also be computed recursively, as demonstrated in the study by Gazi [27]:

$$Z(W_N^{NK-1}) = 2Z\left(W_{\frac{N}{2}}^{k}\right) - [Z\left(W_{\frac{N}{2}}^{k}\right)]^2 \quad (1)$$

where the initial value to preform recursion to be

$$Z(W_1^1) = \alpha \quad (2)$$

whereas, α is the erasure probability of the channel and calculated for the Bhattacharyya parameters:

$$Z(W_N^k) = 1 - Z(W_N^k) \quad (3)$$

The goal of calculating the parameter is to get the maximum value of the probability of channel transmission error. Assume $N = 4$ where N is the transmitted channel numbers of the bits transmitted and $\alpha = 0.5$ by applying the equation our erasure probability will be:

$$Z(W_1^1) = 0.5 \quad (4)$$

For our assumption N=4 will follow the results of the applied as we mentioned in the Eq. (1) for the evaluation at $k = 1, and\ k = 2$ where K is the iteration for calculating the probabilities of the transmitted bits as follow:

$$\text{For } k = 1$$
$$Z(W_4^1) = 2Z(W_2^1) - [Z(W_2^1)]^2 = 2 \times 0.75 - [0.75]^2 = 0.9375 \quad (5)$$

$$Z(W_4^2) = [Z(W_2^1)]^2 = [0.75]^2 = 0.5625 \quad (6)$$

$$k = 2$$
$$Z(W_4^3) = 2Z(W_2^2) - [Z(W_2^2)]^2 = 2 \times 0.25 - [0.25]^2 = 0.4375 \quad (7)$$

$$Z(W_4^2) = [Z(W_2^2)]^2 = [0.25]^2 = 0.0625 \quad (8)$$

The resultant:

$$Z(W_4^i) = [\ 0.9375\ 0.5625\ 0.4375\ 0.0625\ ]$$

which implies that the least probability and largest error in $Z(W_4^4)$. For our assumption, the code rate is 0.5 this requires us to froze 2 bits to utilize the transmission.

Another approach compared to the Bhattacharyya parameter is Reed-Muller codes, which are like polar codes in the sense of generator matrices. Both codes are constructed by selecting rows from a matrix. The selection minimizes the error probability under successive codes. Both codes achieve the capacity of BEC using SC. The goal of using Reed-Muller Codes is to improve error correction performance [38].

The construction of Polar codes using RM can be described in polar using a length of $N = 2^n$ with k and $R = \frac{k}{N}$ following the generator matrix multiplication of $x = uG^{*n}$ Both approaches can be used in Polar Codes and effectively Arikan proposed using Bhattacharyya Parameter for the ease of calculation.

Polar Codes are used based on the polarization of the channel [36]. The concept of the Polar Codes is to ascertain the set of unreliable channels that will cause an increase in the bit error rate. These sets are called the frozen bits [39]. A variant of successive cancellation decoder is utilized in Polar Code base on a folding channel [40]. Defining multiple folding operations or using the same SCD will result in the same performance of the multiple successive cancellations [41]. For better performance compared to other techniques, systematic Polar Codes were proposed by Arikan to improve the bit error rate (BER) [42]. For efficient encoders in the implementation of Polar Codes, systematic polar codes are used with ($N \log N$) for the complexity of the implementation [43].

In section 1.2.3, we elaborated on determining of the frozen bit method; however, this technique will be utilized for encoding process for an example of both encoding and decoding process, using $N = 8$ Encoder happens in M where it is the encoded bits and happened when we multiply our bits with matrix generator.

$$x' = u' \times G$$

which is the information sequence and the arrangement of the frozen bit is $K = 4$ and the information bits are [1001] to get encoded bits M. The code rate used here is 1/2 there for polar encoder structure is depicted as shown in Figure 2.

$$x1 = u1 \oplus u2 \oplus u3 \oplus u4 \oplus u5 \oplus u6 \oplus u7 \oplus u8$$

$$x2 = u5 \oplus u6 \oplus u7 \oplus u8$$

$$x3 = u3 \oplus u4 \oplus u7 \oplus u8$$

$$x4 = \oplus u7 \oplus u8$$

$$x5 = u2 \oplus u4 \oplus u6 \oplus u8$$

$$x6 = u6 \oplus u8$$

$$x7 = \oplus u4 \oplus u8$$

$$x8 = \oplus u8$$

The output for $M = 8$ which are the encoded bits [00001111]. Mainly these encoded bits with the air transmission noise can be affected during transmission; however, we will assume the channel has no noise in it and we will perform decoding using successive cancelation decoding technique.

We know our frozen bits; therefore, we need to calculate the LR of non-frozen bits. This can be done by using formula to determine xx by finding the Likely LR LLR's. To perform decoding let's summaries the following like the value of $\alpha = 0.5$ and $N = 8$ from our example so we determine and use the sorting vector.

$$\pi 8 = [8\ 7\ 6\ 5\ 4\ 3\ 2\ 1]$$

As we explained in chapter of determination the frozen bits, we know location of the frozen bits as it's can be used as parity bits and error correction

$$d = [0^*\ 0^*\ 0^*\ 1\ 0^*\ 1\ 1\ 1]$$

where, $0*$ are the frozen bits. Data vectors are none zeros

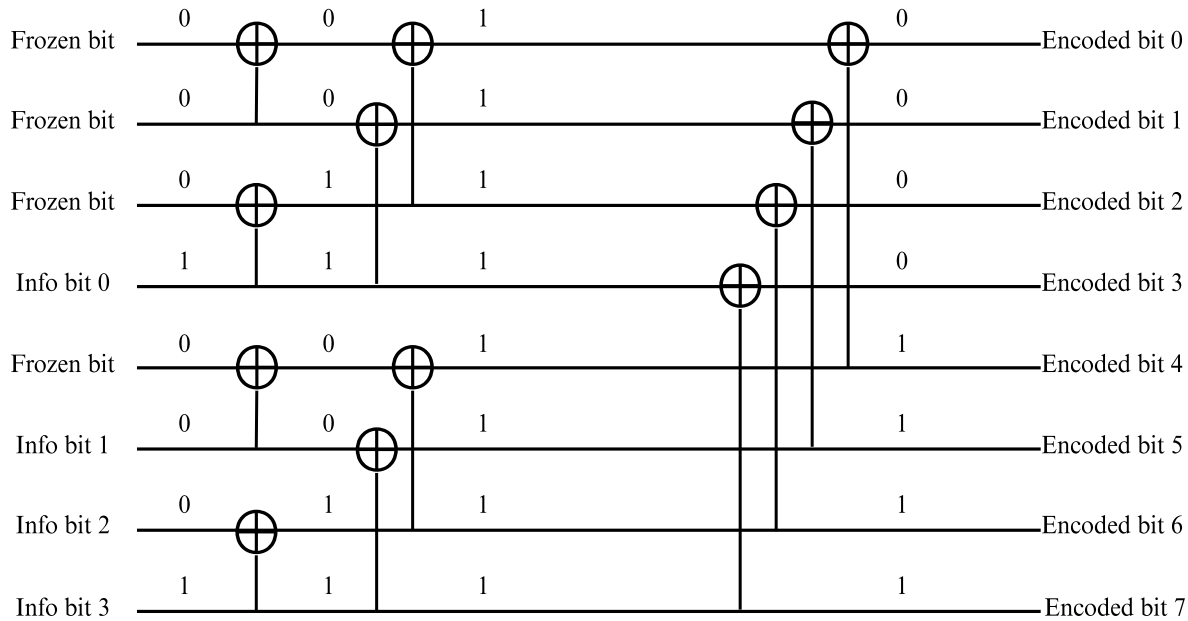

Figure 2. Eight bit polar code encoder

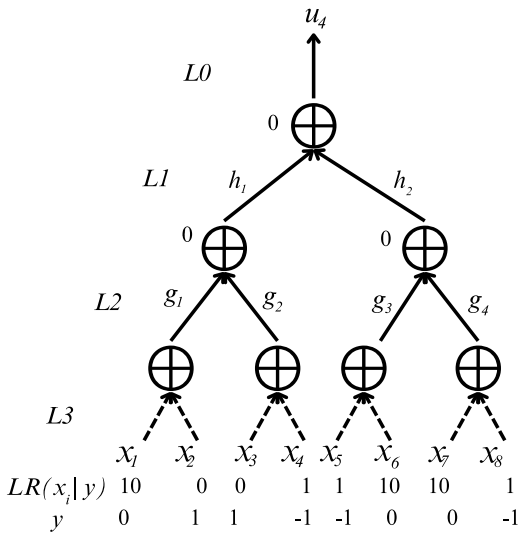

Figure 3. Eight bit polar code decoder

$$d = [0^* \; 0^* \; 0^* \; 1 \; 0^* \; 1 \; 1 \; 1]$$

Therefore, the reverse of encoding shall be the same for decoding, illustrated in Figure 3.

$$u' = d'G = [0 \; 0 \; 0 \; 1 \; 0 \; 1 \; 1 \; 1]$$

Assume the received vector for an Additive White Gaussian Noise (AWGN)AWGN is the following

$$y' = [0 \; 1 \; 1 - 1 - 1 \; 0 \; 0 - 1]$$

We shall decode it by using the decoding tree. To decode, the first step is to calculate the l LR. So, for the first bits, let's decode $u4$

$$LR(x_1|y_1) = 10 \; LR(x_2|y_2) = 0 \;\; LR(x_3|y_3) = 0 \; LR(x_4|y_4) = 1$$
$$LR(x_5|y_5) = 1 \; LR(x_6|y_6) = 0 \;\; LR(x_7|y_7) = 10 \; LR(x_8|y_8) = 1$$

which can be written as

$$L_3 = [10 \; 0 \; 0 \; 1 \; 1 \; 10 \; 10 \; 1]$$

As we know, the first 3 bits are frozen bits

$$(u') = [u_1 = u_2 = u_3 = 0]$$

We can distribute the first decoded to the tree, then we can decode the data in u4, and the likelihood in level 2 can be calculated as follows which can be written as:

$$LR(g_1) = \frac{1+LR(x_1)LR(x_2)}{LR(x_1)+LR(x_2)} \; LR(g_2) = \frac{1+LR(x_3)LR(x_4)}{LR(x_3)+LR(x_4)}$$

$$LR(g_3) = \frac{1+LR(x_5)LR(x_6)}{LR(x_5)+LR(x_6)} \;\; LR(g_4) = \frac{1+LR(x_7)LR(x_8)}{LR(x_7)+LR(x_8)}$$

Moreover, likelihoods for level one will be calculated as follows:

$$LR(g_1) = 0.1 \; LR(g_2) = 1 \;\; LR(g_3) = 1 \;\; LR(g_4) = 1$$

Leading to the first value of likelihood of 1 and 2, we can write the vector as follows:

$$L_2 = [0.1 \; 1 \; 1 \; 1]$$
$$LR(h_1) = (LR(g_1))^{1-2\times 0} LR(g_2) \rightarrow LR(h_1) = LR(g_1)LR(g_2)$$
$$LR(g_1) = (LR(g_3))^{1-2\times 0} LR(g_4) \rightarrow LR(h_2) = LR(g_3)LR(g_4)$$
$$LR(h_1) = 0.1 \; LR(h_2) = 1$$
$$L_2 = [0.1 \; 1 \;]$$

Finally, to the last stage of level zero, which can be calculated as follows:

$$(u_4) = LR(h_1)LR(h_2)$$

Leading to the value

$$LR(u_4) = 0.1$$

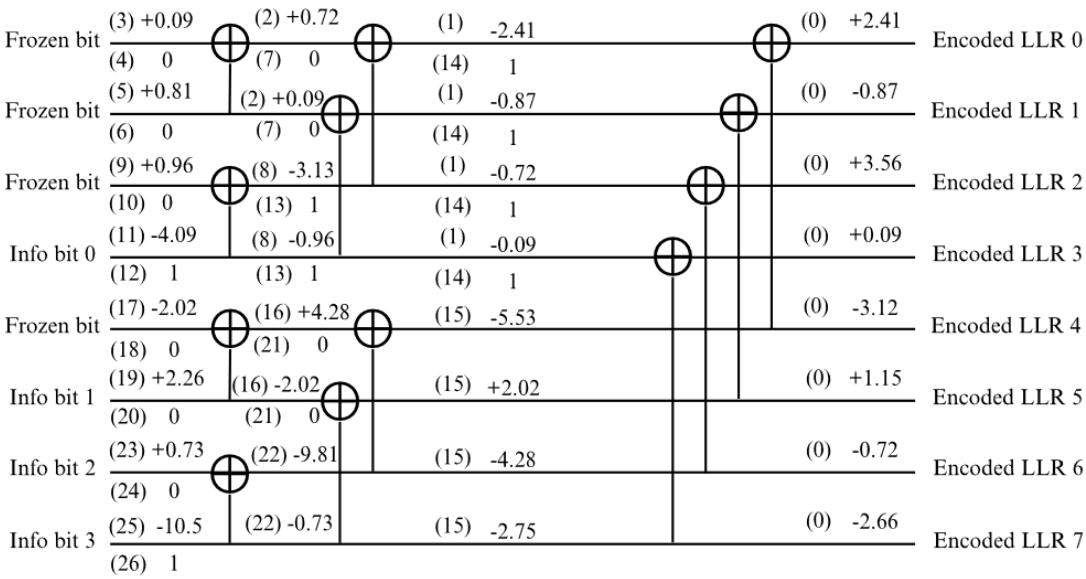

Figure 4. Eight bit polar code decoder resultant

Now, the last step is using the decoding logic operation as shown in Figure 4. We can decide that, if the first decoded information bit for our example $u4$ is 1 or 0, based on our last value with the frozen bits, the decoded bit can now be written as follows:

$$(u_i) = \begin{cases} 0 \; if \; L(u_i) \geq 1 \\ 1 \; otherwise \end{cases}$$

The process will be continued on all data vectors of ui which received from y'.

The resultant output for the case with the arrangement of frozen bits is used to set our set of M = 8 encoded LLRs into the K = 4 we recovered information bits [1001]. The LLRs obtained using the f function.

$$(x') = f(x_a, x_b)$$

and g functions are shown above each connection. The bits obtained using the partial sum computations of (4) and (5) are shown below each connection. The accompanying numbers in pare paper identify the step of the SC decoding process where the corresponding LLR or bit becomes available.

A major aspect of developing the Polar Coding rate in the non-orthogonal multiple access has been proved to increase the multiple-access achievable rate [44] compared to turbo code and LDPC. The Polar code showed an efficient construction in high-order modulation. This approach was estimated in the LM-rate while using AWGN in the demapping technique [28]. This can be considered a new area of research.

To the best of our knowledge, two research papers have shown the performance of using FEC in LPWAN. The first work has evaluated the latency performance using a rete-less polar code with a fixed rate in an LPWAN [45]. The work does not focus on enhancing error rate performance and data rate transmission. The other work used FSK-Turbo codes in LPWAN [46] to enhance the error rate performance. However, FSK-Turbo has high complexity. FSK Turbo uses Frequency Shift Keying, which helps in making high transmission by using two frequencies to transmit two bits but consumes more bandwidth. On the other hand, Polar Code uses BPSK, which uses phase-shifting carrier frequency, which is not affect the bandwidth as FSK [47].

3. METHODOLOGY

The current section delineates the outcomes of the application of our model, illustrating its capacity for potential range determination and coexistence in a Chirp Spread Spectrum (CSS)-based network. Prior to approximating the potential range, it is imperative to derive a closed-form expression for the Bit Error Rate (BER) of CSS symbols, contingent upon the varying spreading factors. Accordingly, a simulation entailed the generation of 10,000 symbols for each Signal-to-Noise Ratio (SNR) value, followed by their decoding through the methodology explicated in Background.

The data points acquired from this simulation were then incorporated into MATLAB's curve fitting toolbox and 5G libraries for Polar Codes and LPWAN to simulate the process. We also facilitate the derivation of an empirical Bit Error Rate (BER) curve for CSS. This process necessitates defining the variables that constitute the foundational parameters of our simulation, as mentioned in Table 3. One of the primary objectives of this research is to construct a graphical representation of the BER for Long Range (LoRa) communication, enabling a comparative analysis between the standard LoRa Alliance specifications and an enhanced LPWAN LoRa employing Polar Codes.

Table 3. Code attribute

Definition	Attribute	Value
Spreading Factor SF	SF	7:12
Bandwidth BW	BW	125khz, 250khz, 500khz
Sampling Frequency Fs	Fs	125khz, 250khz, 500khz
Total Bits	Total_Bits	27720
Signal to Noise Ratio dB	SNR_dB	(- 40db: 5db)
number of iterations	num_iter	100
LoRa modulated bits	E	110
Decoded bits	K	220
AWGN	AWGN	
Number of Samples	Num_samples	10000
Bit Error Rate	BER	
Poly24c	Poly24c	CRC24

The inception of this definition involves specifying the bandwidth, which, for our initial conditions, is set at 125 kHz. This bandwidth yields a chip rate of 125,000 chips per second. Considering a spreading factor of 7, each symbol encapsulates 7 bits of information, resulting in a total of $(2^7 = 128)$ chips per symbol. To comprehensively address all possible spreading factors pertinent to our CSS model, the simulation encompasses a total of 27,720 bits. The Symbol Rate, a crucial parameter in our analysis, is deduced via the subsequent equation provided in the research.

$$T_s = \frac{B}{2^{SF}}$$

Moreover, each spreading factor will define a new symbol rate based on our spreading factor range we choose during the simulation. The chip rate is always higher than the symbol rate. To calculate the data rate, we can use this equation.

$$R_b\left(\frac{bits}{sec}\right) = SF \times \frac{B}{2^{SF}} \times \frac{4}{4+Code\ Rate\ (CR)}$$

Note that the Code rate ranges from 1-4. Since the chip rate is the same as the bandwidth, we can calculate the chip duration.

$$T_c = \frac{1}{B}$$

To calculate the symbol duration is the inverse of the symbol rate as shown in the equation.

$$T_s(\text{sec}) = \frac{2^{SF}}{B}$$

The impact of having several spreading factors is examined to elucidate their effects. For example, an increase in the spreading factor by one lead to a doubling of the symbol duration sweep time. Simultaneously, the bit rate will be approximately half compared to the previous SF, but the time any message transmission will increase. In our case, LoRa

needs a larger spreading factor for long-range transmission, especially if the signal becomes weaker due to interference.

The code first generates all attributes and bits for the signal to be transmitted. Therefore, the noise ratio ranges between -40db to 5db and by applying the following equation.

$$SNR = 10\ log_{10}\ (\frac{Signal}{Noise})$$

Moving forward, after generating the bits, we shall encode them using Polar Codes before modulating the output through chirp spread spectrum. For Polar Codes, we use the 5G Polar Codes Matlab tool with the following definition. As random bits are generated, CRC is computed and appended to the message with data. Rate matching is performed to transmit the bits to extract a set of bits to be transmitted at any given time. Moreover, AWGN is added to the signal to simulate a signal transmitted with noise in the air. For decoding, we are using Successive cancellation List decoding.

4. SYSTEM MODEL

The accompanying diagram shown in Figure 5 and the table detail the implementation process of our novel method, from the initial bit intended for transmission to the final reception of bits at the receiver's end. As depicted, we append a Cyclic Redundancy Check (CRC) to detect any errors, and this is succeeded by the Polar Code encoder that encodes the bits meant for transmission. To minimize the potential for logical errors associated with the polar encoder, we employ Grey coding to represent the bits. Furthermore, prior to transmission, the bits undergo modulation via Chirp Spread Spectrum (CSS) technology, as elaborated in section 1.2.4, which finds application in Low-Power Wide-Area Network (LPWAN) technologies. To emulate the process of transmission through the air, an AWGN channel is utilized in our simulation. Upon receiving the bits, the demodulation is carried out using CSS, followed by the remapping and decoding of the bits with the Polar Code decoder. Finally, we strip away the CRC to retrieve the original transmitted bits.

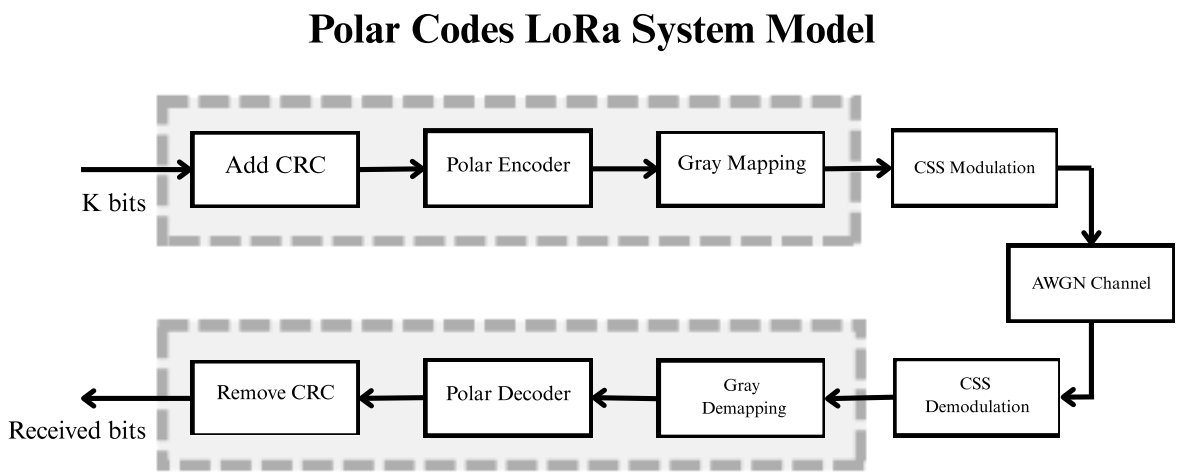

Figure 5. System model diagram

5. RESULT AND DISCUSSIONS

Throughout my research, the study thoroughly investigated the impact of Bit Error Rate (BER) on the quality and reliability of communication systems employing CSS encoded with Polar Codes in an AWGN environment. The BER serves as a crucial metric for assessing the system's ability to preserve the integrity of data transmission amidst noise and is a direct reflection of system performance. The combination of CSS, which offers resilience against interference, and Polar Codes, renowned for their error correction proficiency, is postulated to enhance system robustness—especially under the influence of AWGN, which is the standard noise model for communication channels.

My findings reveal in Figure 6 that, within a 125 kHz bandwidth, Polar Code with spreading factor (SF) variation significantly influences BER performance. It is evident that higher SFs, particularly LoRa/Polar SF12 immune the noise from effecting the bits transmitted, the robustness of the channel benefits of the larger spreading factors tend to disappear as the payload size grows however Polar Codes as we explained in Section 2 tends to maximize the rate at which information can be transmitted. which demonstrate superior BER performance compared to lower SFs such as SF6 and SF7 in the same coding technique which we used, suggesting that increased SF is beneficial for noise mitigation at this bandwidth.

Upon comparison with the baseline LoRa modulation, we can see significant difference in energy of almost 5 db. The enhanced scheme integrating Polar Codes manifests a remarkable reduction in BER at equivalent SNRs, showcasing a pronounced enhancement in transmission reliability. Nonetheless, this advancement is achieved at the expense of elevated computational complexity and processing time.

When progressing to wider bandwidths of 250 kHz as shown in Figure 7, the data indicates that the BER improves with increased bandwidth. The SF12 in particular exhibits robust performance as we explained before in the 125 kHz, implying that a higher bandwidth can deliver lower BER in normal LPWAN scheme, at the cost of increased computation compared to the enhanced technique. Despite the additional computational requirements, my coding scheme maintains a superior BER profile. Since Polar Codes maximize the transmission rate. However, the difference of 4db is showed

when compared to standard LoRa modulation amongst all SFs tested.

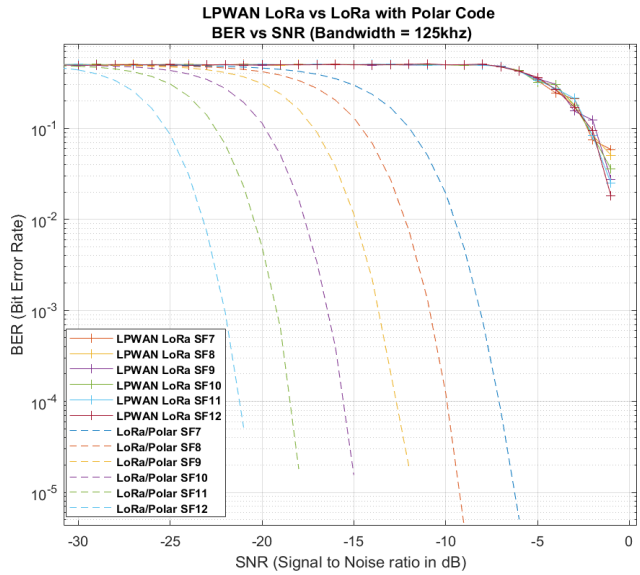

Figure 6. BER of LPWAN LoRa Vs LPWAN Polar Code at 125khz

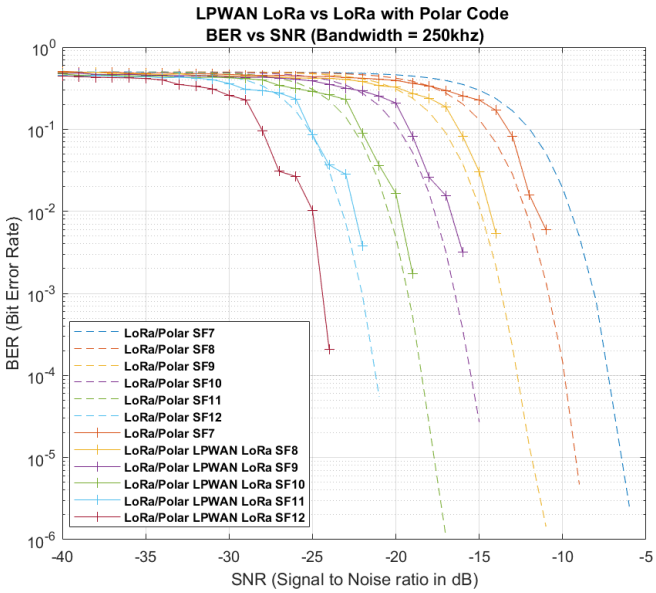

Figure 7. BER of LPWAN LoRa Vs LPWAN Polar Code at 250khz

Upon examining data associated with increased bandwidths, specifically at the 250 kHz level, there is a discernible enhancement in Bit Error Rate (BER) performance concomitant with the bandwidth expansion. The strong performance, suggesting that higher bandwidths are effective in reducing BER as in standard LPWAN configurations with Spreading Factor 12. This reduction in BER, however, necessitates a trade-off in the form of elevated computational complexity when contrasted with the refined methodology employed in the enhanced coding technique Polar Codes with LPWAN.

Despite this trade-off, the coding scheme I have devised consistently offers a superior BER profile, maintaining its performance compared to the conventional LoRa modulation technique. This comparison is quantified by a notable 4 dB in BER across the board for all other spreading factors tested. This led us to test a higher bandwidth to observe more resilient results.

The analysis of bandwidths at 500 kHz reveals a notable trend: as bandwidth increases, there is a corresponding improvement in Bit Error Rate (BER) for both Spreading Factor SF12 and SF11 within standard LoRa compared to the newly enhanced LoRa/Polar scheme and compared to the other bandwidth analysis. This finding extends to all tested spreading factors when compared with the conventional LoRa system, suggesting that a wider bandwidth is conducive to achieving a lower BER in a typical LPWAN configuration. This benefit, however, comes at the expense of heightened computational demands, which are intrinsic to the enhanced scheme.

Despite the greater computational load, the innovative coding scheme I have developed is not far than the BER profile of the standard LoRa approach. This performance is quantified by a 6 dB improvement across all the spreading factors that were evaluated. This differential indicates that the new scheme can maintain a lower BER even in conditions that are conventionally challenging for standard LoRa modulations.

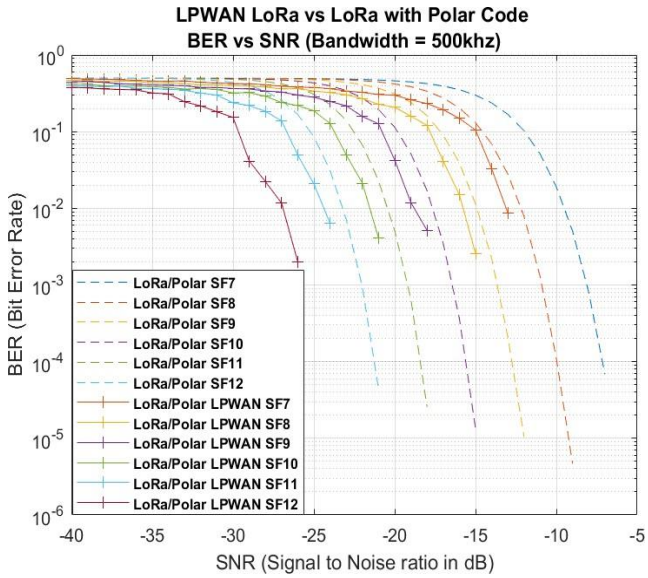

Figure 8. BER of LPWAN LoRa Vs LPWAN Polar Code at 500khz

The simulation in Figure 8 establishes that increasing data will also help in reducing the BER as this have been proven in Polar Codes adding to it the integration of Chirp Spread Spectrum (CSS) with Polar Codes significantly enhances the BER performance when contrasted with the conventional LoRa modulation in low data rate such as mentioned above in the 125khz compared to 250khz and 500khz. However, even with high data rate with computational complexity of polar code the enhanced scheme can almost achieve what standard LoRa apply. This synergy between the robust modulation technique and the advanced error-correction coding demonstrates a clear improvement in signal reliability and data integrity, particularly in the presence of AWGN. The findings show that there is a potential of this combined approach to elevate the quality of communication systems, rendering it a promising solution for applications requiring high levels of transmission fidelity.

In summary, my research confirms that my Polar Code-enhanced with CSS modulation scheme significantly surpasses the standard LoRa scheme in low data rate in BER

performance compared to higher bandwidths and SFs. The enhanced reliability of data transmission with my scheme is essential for applications that demand high levels of communication integrity. The trade-off, however, is the requirement for more computational resources and time, a consideration that is crucial in the context of low-power, wide-area network applications where efficiency and resource optimization are key.

6. CONCLUSIONS

In the presented paper, we approach the study of Polar Codes with an optimistic hypo paper regarding their potential to substantially mitigate the bit error rate (BER) within communication systems. Polar Codes are posited as a promising coding technique capable of enhancing reliability by decreasing the BER, a metric of critical importance in the evaluation of communication systems. We put forth a novel decoding scheme tailored to LoRa LPWAN applications, asserting that our approach can significantly curtail the BER without incurring prohibitive increases in computational complexity.

In the analysis of communication systems that employ Chirp Spread Spectrum (CSS) technology, several critical insights emerge that merit particular attention. The first of these insights is the effect of Spreading Factors to the modulation technique, which increase the robustness against interference, an attribute largely attributable to the technique of spreading the signal's spectral components. As a result of this expansive spectral footprint, CSS signals are more vulnerable to the cumulative effect of multiple interfering sources, which can depress the Signal-to-Interference-plus-Noise Ratio (SINR) below the level required for reliable detection and decoding. The second insight revolves around the complexity of Polar Codes in coding technique and the computational time to transmit data, adding a pivotal relationship between the budgetary constraints and the capacity of the bandwidth. The third insight concerns the trade-offs associated with employing multiple spreading factors to augment system throughput. The use of a variety of spreading factors allows for greater flexibility in adjusting the data rate and range of communication.

To summarize, these insights underscore the complexity and interdependence of factors that govern the performance of CSS-based communication systems. From the interference-resistant nature of CSS to the economic-bounded bandwidth considerations, and the nuanced selection of spreading factors for throughput optimization, each element plays an integral role in the design and functionality of contemporary communication networks. Understanding these dynamics is crucial for advancing the development of efficient, cost-effective, and resilient communication technologies that can thrive in the face of diverse and challenging operational environments.

7. CONTRIBUTION AND FUTURE WORK

In this discourse, we delve into an analysis of the physical layer (PHY) data transmission channel within the framework of LPWAN technology. Our comprehensive performance analysis, supported by empirical results, corroborates the assertion that the proposed decoding scheme significantly enhances transmission reliability for users of LoRa networks. In prospect, our prospective research endeavors will pivot towards the practical application and validation of our theoretical work. This will entail the deployment and real-time assessment of our enhanced decoding scheme within Software-Defined Radio (SDR) hardware, thereby translating our academic contributions into tangible improvements in LPWAN PHY layer communications.

ACKNOWLEDGMENT

The authors extend their appreciation to Ongoing Research Funding program, (ORF-2025-636), King Saud University, Riyadh, Saudi Arabia.

The authors wish to thank King Abdulaziz for Science and Technology for allowing them to use their labs.

REFERENCES

[1] Porkodi, R., Bhuvaneswari, V. (2014). The internet of things (IOT) applications and communication enabling technology standards: An overview. In 2014 International Conference on Intelligent Computing Applications, Coimbatore, India, pp. 324-329. https://doi.org/10.1109/ICICA.2014.73

[2] Reynders, B., Pollin, S. (2016). Chirp spread spectrum as a modulation technique for long range communication. In 2016 Symposium on Communications and Vehicular Technologies (SCVT), Mons, Belgium, pp. 1-5. https://doi.org/10.1109/SCVT.2016.7797659

[3] Kartakis, S., Choudhary, B.D., Gluhak, A.D., Lambrinos, L., McCann, J.A. (2016). Demystifying low-power wide-area communications for city IoT applications. In Proceedings of the Tenth ACM International Workshop on Wireless Network Testbeds, Experimental Evaluation, and Characterization, New York, USA, pp. 2-8. https://doi.org/10.1145/2980159.2980162

[4] Centenaro, M., Vangelista, L., Zanella, A., Zorzi, M. (2016). Long-range communications in unlicensed bands: The rising stars in the IoT and smart city scenarios. IEEE Wireless Communications, 23(5): 60-67. https://doi.org/10.1109/MWC.2016.7721743

[5] Mekki, K., Bajic, E., Chaxel, F., Meyer, F. (2019). A comparative study of LPWAN technologies for large-scale IoT deployment. ICT Express, 5(1): 1-7. https://doi.org/10.1016/j.icte.2017.12.005

[6] Nikoukar, A., Raza, S., Poole, A., Güneş, M., Dezfouli, B. (2018). Low-power wireless for the internet of things: Standards and applications. IEEE Access, 6: 67893-67926. https://doi.org/10.1109/ACCESS.2018.2879189

[7] Guibene, W., Nowack, J., Chalikias, N., Fitzgibbon, K., Kelly, M., Prendergast, D. (2017). Evaluation of LPWAN technologies for smart cities: River monitoring use-case. In 2017 IEEE Wireless Communications and Networking Conference Workshops (WCNCW), San Francisco, CA, USA, pp. 1-5. https://doi.org/10.1109/WCNCW.2017.7919089

[8] Ratasuk, R., Mangalvedhe, N., Ghosh, A. (2015). Overview of LTE enhancements for cellular IoT. In 2015 IEEE 26th annual international symposium on personal, indoor, and mobile radio communications (PIMRC), Hong Kong, China, pp. 2293-2297.

https://doi.org/10.1109/PIMRC.2015.7343680
[9] Roth, Y., Doré, J.B., Ros, L., Berg, V. (2018). The Physical Layer of Low Power Wide Area Networks: Strategies, Information Theory's Limit and Existing Solutions. Advances in Signal Processing: Reviews, Vol. 1, Book Series.
[10] Patel, D., Won, M. (2017). Experimental study on low power wide area networks (LPWAN) for mobile Internet of Things. In 2017 IEEE 85th vehicular technology conference (VTC Spring), Sydney, NSW, Australia, pp. 1-5. https://doi.org/10.1109/VTCSpring.2017.8108501
[11] Carlsson, A., Kuzminykh, I., Franksson, R., Liljegren, A. (2018). Measuring a LoRa network: Performance, possibilities and limitations. In Internet of Things, Smart Spaces, and Next Generation Networks and Systems, pp. 116-128. https://doi.org/10.1007/978-3-030-01168-0_11
[12] Sinha, R.S., Wei, Y., Hwang, S.H. (2017). A survey on LPWA technology: LoRa and NB-IoT. ICT Express, 3(1): 14-21. https://doi.org/10.1016/j.icte.2017.03.004
[13] Paredes, W.D., Kaushal, H., Vakilinia, I., Prodanoff, Z. (2023). LoRa technology in flying ad hoc networks: A survey of challenges and open issues. Sensors, 23(5): 2403. https://doi.org/10.3390/s23052403
[14] Sigfox World Coverage (2025). www.sigfox.com/en/coverage/.
[15] Sigfox One Network a Billion Dreams. M2M and IoT Redefined Through Cost Effective and Energy Optimized Connectivity. https://lafibre.info/images/3g/201302_sigfox_whitepaper.pdf.
[16] Jouhari, M., Saeed, N., Alouini, M.S., Amhoud, E.M. (2023). A survey on scalable LoRaWAN for massive IoT: Recent advances, potentials, and challenges. IEEE Communications Surveys & Tutorials, 25(3): 1841-1876. https://doi.org/10.1109/COMST.2023.3274934
[17] Apat, H.K., Nayak, R., Sahoo, B. (2023). A comprehensive review on Internet of Things application placement in fog computing environment. Internet of Things, 23: 100866. https://doi.org/10.1016/j.iot.2023.100866
[18] Math, S., Tam, P., Lee, A., Kim, S. (2023). A NB-IoT data transmission scheme based on dynamic resource sharing of MEC for effective convergence computing. Personal and Ubiquitous Computing, 27(3): 1065-1075. https://doi.org/10.1007/s00779-020-01449-5
[19] Muteba, K.F., Djouani, K., Olwal, T. (2022). 5G NB-IoT: Design, considerations, solutions and challenges. Procedia Computer Science, 198: 86-93. https://doi.org/10.1016/j.procs.2021.12.214
[20] Kanj, M., Savaux, V., Le Guen, M. (2020). A tutorial on NB-IoT physical layer design. IEEE Communications Surveys & Tutorials, 22(4): 2408-2446. https://doi.org/10.1109/COMST.2020.3022751
[21] Sisinni, E., Mahmood, A. (2021). Wireless communications for industrial Internet of Things: The LPWAN solutions. Wireless Networks and Industrial IoT: Applications, Challenges and Enablers, pp. 79-103. Springer, Cham. https://doi.org/10.1007/978-3-030-51473-0_5
[22] Migabo, E.M., Djouani, K.D., Kurien, A.M. (2020). The narrowband Internet of Things (NB-IoT) resources management performance state of art, challenges, and opportunities. IEEE Access, 8: 97658-97675. https://doi.org/10.1109/ACCESS.2020.2995938
[23] Lalle, Y., Fourati, L. C., Fourati, M., & Barraca, J. P. (2019, December). A comparative study of LoRaWAN, SigFox, and NB-IoT for smart water grid. In 2019 Global Information Infrastructure and Networking Symposium (GIIS), Paris, France, pp. 1-6. https://doi.org/10.1109/GIIS48668.2019.9044961
[24] LoRa World Coverage (2017). https://lora-alliance.org/.
[25] Arikan, E. (2011). Systematic polar coding. IEEE Communications Letters, 15(8): 860-862. https://doi.org/10.1109/LCOMM.2011.061611.110862
[26] Arikan, E. (2009). Channel polarization: A method for constructing capacity-achieving codes for symmetric binary-input memoryless channels. IEEE Transactions on Information Theory, 55(7): 3051-3073. https://doi.org/10.1109/TIT.2009.2021379
[27] Kahraman, S., Viterbo, E., Celebi, M.E. (2014). Folded successive cancelation decoding of polar codes. In 2014 Australian Communications Theory Workshop (AusCTW), Sydney, NSW, Australia, pp. 57-61. https://doi.org/10.1109/AusCTW.2014.6766428
[28] Gazi, O. (2019). Information theory perspective of polar codes and polar encoding. In: Polar Codes. Springer Topics in Signal Processing, Springer, Singapore, vol. 15. https://doi.org/10.1007/978-981-13-0737-9_1
[29] Hernandez, D.M., Peralta, G., Manero, L., Gomez, R., Bilbao, J., Zubia, C. (2017). Energy and coverage study of LPWAN schemes for Industry 4.0. In 2017 IEEE International Workshop of Electronics, Control, Measurement, Signals and Their Application to Mechatronics (ECMSM), Donostia, Spain, pp. 1-6. https://doi.org/10.1109/ECMSM.2017.7945893
[30] LoRa Alliance Technical Committee. (2017). LoRaWAN® Specification v1.1. https://resources.lora-alliance.org/technical-specifications/lorawan-specification-v1-1.
[31] Zakariyya, R.S., Jewel, K.H., Fadamiro, A.O., Famoriji, O.J., Lin, F. (2020). An efficient polar coding scheme for uplink data transmission in narrowband internet of things systems. IEEE Access, 8: 191472-191481. https://doi.org/10.1109/ACCESS.2020.3032636
[32] Mainwaring, A., Culler, D., Polastre, J., Szewczyk, R., Anderson, J. (2002). Wireless sensor networks for habitat monitoring. In Proceedings of the 1st ACM International Workshop on Wireless Sensor Networks and Applications, Atlanta Georgia, USA, pp. 88-97. https://doi.org/10.1145/570738.570751
[33] Krishnamurthy, L., Adler, R., Buonadonna, P., Chhabra, J., Flanigan, M., Kushalnagar, N., Nachman, L., Yarvis, M. (2005). Design and deployment of industrial sensor networks: Experiences from a semiconductor plant and the North Sea. In Proceedings of the 3rd International Conference on Embedded Networked Sensor Systems, San Diego California, USA, pp. 64-75. https://doi.org/10.1145/1098918.1098926
[34] Woodard, J.P., Hanzo, L. (2000). Comparative study of turbo decoding techniques: An overview. IEEE Transactions on Vehicular Technology, 49(6): 2208-2233. https://doi.org/10.1109/25.901892
[35] Neumann, P., Montavont, J., Noel, T. (2016). Indoor deployment of low-power wide area networks (LPWAN): A LoRaWAN case study. In 2016 IEEE 12th International Conference on Wireless and Mobile Computing, Networking and Communications (WiMob), New York, USA, pp. 1-8.

https://doi.org/10.1109/WiMOB.2016.7763213
[36] Tahir, B., Schwarz, S., Rupp, M. (2017). BER comparison between Convolutional, Turbo, LDPC, and Polar codes. In 2017 24th International Conference on Telecommunications (ICT), Limassol, Cyprus, pp. 1-7. https://doi.org/10.1109/ICT.2017.7998249
[37] Ali, M.M., Hashim, S.J., Chaudhary, M.A., Ferré, G., Rokhani, F.Z., Ahmad, Z. (2023). A reviewing approach to analyze the advancements of error detection and correction codes in channel coding with emphasis on LPWAN and IoT systems. IEEE Access, 11: 127077-127097. https://doi.org/10.1109/ACCESS.2023.3331417
[38] Arikan, E. (2008). A performance comparison of polar codes and Reed-Muller codes. IEEE Communications Letters, 12(6): 447-449. https://doi.org/10.1109/LCOMM.2008.080017
[39] Vangala, H., Viterbo, E., Hong, Y. (2015). A comparative study of polar code constructions for the AWGN channel. arXiv preprint arXiv:1501.02473. https://doi.org/10.48550/arXiv.1501.02473
[40] Sun, H., Wang, Y., Tian, R., Zhao, H. (2020). A nearly optimal method of polar code constructions for the AWGN channel. IEEE Access, 9: 17266-17274. https://doi.org/10.1109/ACCESS.2020.3047127
[41] Vangala, H., Hong, Y., Viterbo, E. (2015). Efficient algorithms for systematic polar encoding. IEEE Communications Letters, 20(1): 17-20. https://doi.org/10.1109/LCOMM.2015.2497220
[42] Liu, Y., Qin, Z., Elkashlan, M., Ding, Z., Nallanathan, A., Hanzo, L. (2017). Nonorthogonal multiple access for 5G and beyond. Proceedings of the IEEE, 105(12): 2347-2381. https://doi.org/10.1109/JPROC.2017.2768666
[43] Bocherer, G., Prinz, T., Yuan, P., Steiner, F. (2017). Efficient polar code construction for higher-order modulation. In 2017 IEEE Wireless Communications and Networking Conference Workshops (WCNCW), San Francisco, USA, pp. 1-6. https://doi.org/10.1109/WCNCW.2017.7919039
[44] Vangala, H., Viterbo, E., Hong, Y. (2015). Polar Coding Algorithms in MATLAB. Monash. https://ecse.monash.edu/staff/eviterbo/polarcodes.html.
[45] Yu, Y., Mroueh, L., Vivier, G., Terré, M. (2019). Packet recovery latency of a rate-less polar code in low power wide area networks. In 2019 European Conference on Networks and Communications (EuCNC), Valencia, Spain, pp. 10-14. https://doi.org/10.1109/EuCNC.2019.8802011
[46] Roth, Y., Doré, J.B., Ros, L., Berg, V. (2015). Turbo-FSK: A new uplink scheme for low power wide area networks. In 2015 IEEE 16th International Workshop on Signal Processing Advances in Wireless Communications (SPAWC), Stockholm, Sweden, pp. 81-85. https://doi.org/10.1109/SPAWC.2015.7227004
[47] Li, L., Maunder, R.G., Al-Hashimi, B.M., Hanzo, L. (2011). A low-complexity turbo decoder architecture for energy-efficient wireless sensor networks. IEEE Transactions on Very Large Scale Integration (VLSI) Systems, 21(1): 14-22. https://doi.org/10.1109/TVLSI.2011.2177104